

Atomic Data: Calculation, evaluation and integration

R-matrix calculations of Mo I and W I

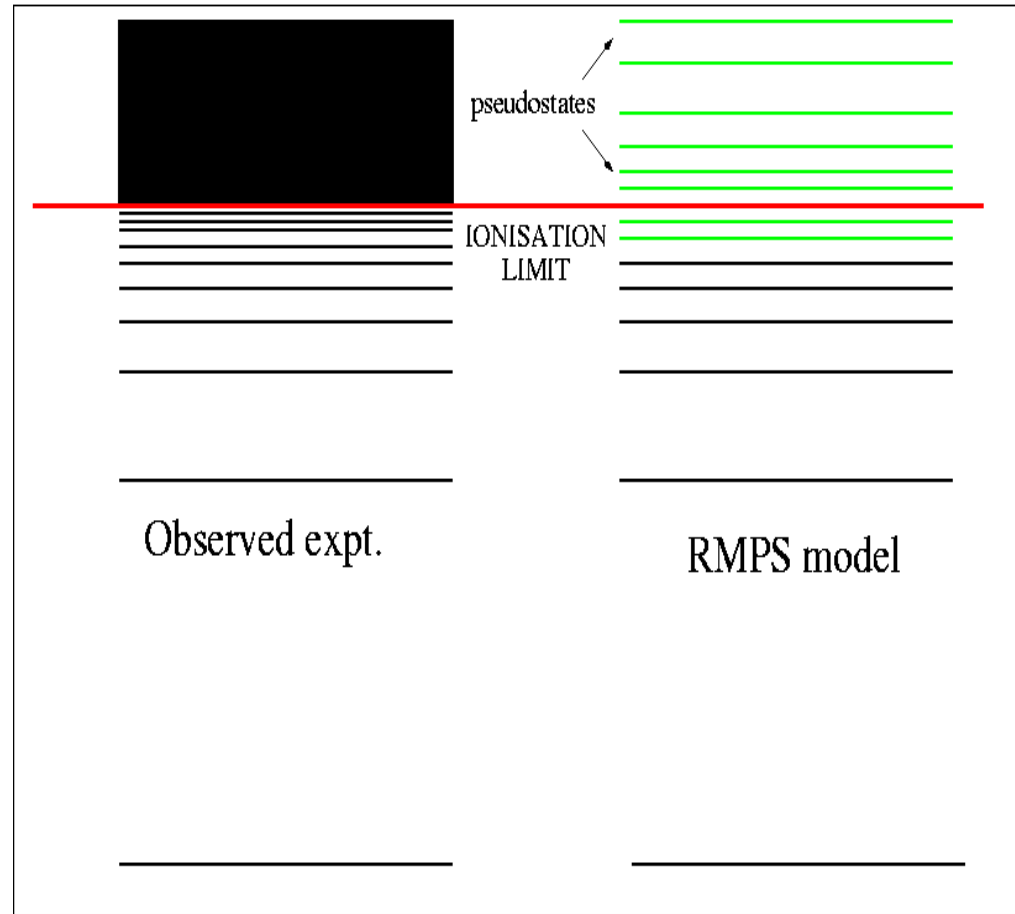
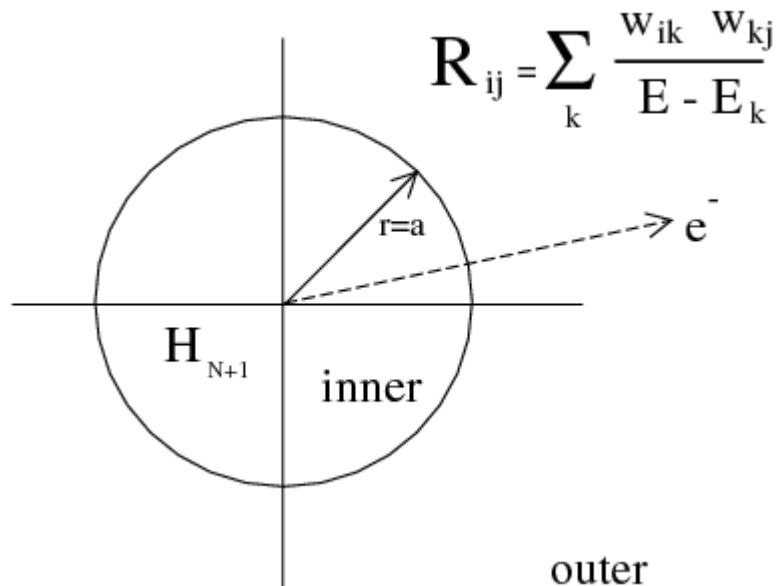
**Connor Ballance
(Queen's University of Belfast)**

September 4-6, Vienna 2017

Overview

- Capabilities of the R-matrix collision group at Queen's Belfast
- Calculations of varying degrees of complexity
(Serial Code ---> Highly parallel codes)
- Evaluation of produced data, error uncertainty
- Integration of results within ADAS (open-adas) database and modelling suite
- Test cases : Mo I (excitation and ionisation)
 : W I (excitation)

R-matrix/R-matrix with Pseudostates (RMPS) review



$$\Psi_k(x_1 \dots x_{N+1}) = A \sum_{ij} c_{ijk} \bar{\Phi}_i(x_1 \dots x_N, \hat{r}_{N+1} \sigma_{N+1}) u_{ij}(r_{N+1}) + \sum_j d_{jk} \phi_j(x_1 \dots x_{N+1})$$

Capabilities

- Most first order electron-impact driven processes

Electron-impact excitation

Electron-impact ionisation

Electron-impact recombination (DR/radiative)

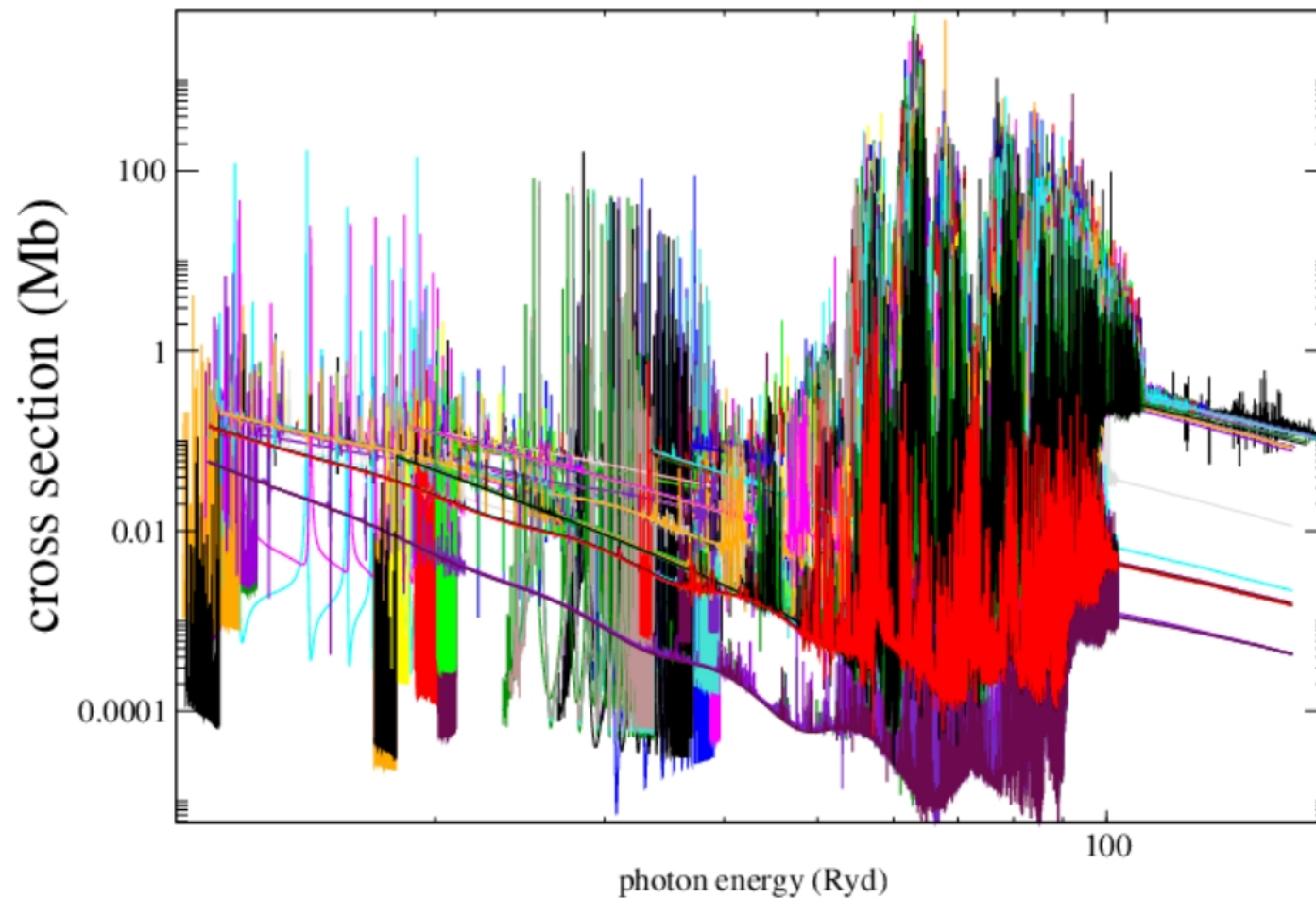
- The codes should cover most of the periodic table, and there are LS coupling (non-relativistic), Breit-Pauli (semi-relativistic) and Dirac R-matrix suites of codes
- Photoionisation is also possible within the codebase, and is currently being used to update stellar opacities(CLOUDY,XSTAR)

High performance computing + scripting = comprehensive data sets

i.e. total photoionisation of every Fe XVII level

$2p^6, 2p^5 nl(5), 2s2p^6 nl(5)$ total photoionisation

$h\nu + \text{Fe XVII}$



Electron-impact excitation and ionization of W^{3+} for the determination of tungsten influx in a fusion plasma

C P Ballance^{1,3}, S D Loch¹, M S Pindzola¹ and D C Griffin²

Published 19 February 2013 • 2013 IOP Publishing Ltd

Journal of Physics B: Atomic, Molecular and Optical Physics, Volume 46, Number 5

[+ Article information](#)

Abstract

Tungsten will be employed as a plasma facing material in the ITER fusion reactor under construction in Cadarache, France; therefore, there is a significant need for accurate electron-impact excitation and ionization data for the ions of tungsten. We report on the results of extensive calculations of ionization and excitation for W^{3+} that are intended to provide the atomic data needed for the determination of impurity influx diagnostics of tungsten in several existing tokamak reactors. The electron-impact excitation rate coefficients for this study were determined using the relativistic *R*-matrix method. The contribution to direct electron-impact ionization was determined using the distorted-wave approximation, the accuracy of which was verified by an *R*-matrix with pseudo states calculation. Contributions to total ionization from excitation autoionization were also generated from the relativistic *R*-matrix method. These results were then employed to calculate values of ionization per emitted photon, or SXB ratios, for four carefully selected spectral lines; these data will allow the determination of impurity influx from tungsten facing surfaces. For the range of densities of importance in the edge region of a tokamak reactor, these SXB ratios are found to be nearly independent of electron density but vary significantly with electron temperature.

Accurate Atomic Structure

+



Electron-impact excitation

+

Ground & metastable
Ionisation

= spectral diagnostics
+ impurity influx
predictions

ATOMIC DATA AND SPECTRAL MODEL FOR Fe II

Manuel A. Bautista¹, Vanessa Fivet^{1,7}, Connor Ballance^{2,8}, Pascal Quinet³, Gary Ferland⁴ ,
Claudio Mendoza⁵ , and Timothy R. Kallman⁶

Published 2015 July 30 • © 2015. The American Astronomical Society. All rights reserved.

[The Astrophysical Journal](#), Volume 808, Number 2



Article PDF

[Figures](#) ▾ [Tables](#) ▾ [References](#) ▾ [Citations](#) ▾ [Article data](#) ▾

+ Article information

Abstract

We present extensive calculations of radiative transition rates and electron impact collision strengths for Fe II. The data sets involve 52 levels from the $3d^7$, $3d^64s$, and $3d^54s^2$ configurations. Computations of A -values are carried out with a combination of state-of-the-art multiconfiguration approaches, namely the relativistic Hartree–Fock, Thomas–Fermi–Dirac potential, and Dirac–Fock methods, while the R -matrix plus intermediate coupling frame transformation, Breit–Pauli R -matrix, and Dirac R -matrix packages are used to obtain collision strengths. We examine the advantages and shortcomings of each of these methods, and estimate rate uncertainties from the resulting data dispersion. We proceed to construct excitation balance spectral models, and compare the predictions from each data set with observed spectra from various astronomical objects. We are thus able to establish benchmarks in the spectral modeling of [Fe II] emission in the IR and optical regions as well as in the UV Fe II absorption spectra. Finally, we provide diagnostic line ratios and line emissivities for emission spectroscopy as well as column densities for absorption spectroscopy. All atomic data and models are available online and through the AtomPy atomic data curation environment.

The atomic data has been integrated into many astrophysical databases such as CLOUDY, XSTAR and AtomDB.

Conversion codes exist to convert ADAS formats into the required files needed for above astrophysical modelling codes

Our goal is to produce, high quality atomic data in a timely fashion, so that it may be employed in current, ongoing experimental campaigns.

For example , level resolved Argon Breit-Pauli R-matrix data was used at DIII-D

PAPER

Use of Ar pellet ablation rate to estimate initial runaway electron seed population in DIII-D rapid shutdown experiments

E.M. Hollmann¹, N. Commaux², R.A. Moyer¹, P.B. Parks³, M.E. Austin⁴, I. Bykov¹, C. Cooper³, N.W. Eidietis³, M. O'Mullane⁵, C. Paz-Soldan³ [Show full author list](#)

Published 3 October 2016 • © 2017 IAEA, Vienna

[Nuclear Fusion](#), Volume 57, Number 1



[Article PDF](#)

[Figures](#) ▾ [References](#) ▾

[+ Article information](#)

Abstract

Small (2–3 mm, 0.9–2 Pa · m³) argon pellets are used in the DIII-D tokamak to cause rapid shutdown (disruption) of discharges. The Ar pellet ablation is typically found to be much larger than expected from the thermal plasma electron temperature alone; the additional ablation is interpreted as being due to non-thermal runaway electrons (REs) formed during the pellet-induced temperature collapse. Simple estimates of the RE seed current using the enhanced ablation rate give values of order 1–10 kA, roughly consistent with estimates based on avalanche theory. Analytic estimates of the RE seed current based on the Dreicer formula tend to significantly underestimate it, while estimates based on the hot tail model significantly overestimate it.

Ideally, in some situations the highest accuracy is required, and months of effort are given to the atomic structure and scattering calculation

but in other cases, comprehensive coverage along iso-electronic sequences is more important, and hence a R-matrix script (in perl) was created for this purpose and also for the novice user.

This script is employed to produce data in a format immediately accepted by ADAS (adf04). This well-prescribed format can (and has) been converted to other database formats such as CLOUDY.

ADAS adf04 : helike_cb12#o6.dat

```
File Edit View Search Tools Documents Help
helike_cb12#o6.dat
0 + 6 8 7 5963164.( )
1 1S2 (1)0( 0.0) 0.0
2 1S1 2S1 (3)0( 1.0) 4526947.0
3 1S1 2P1 (3)1( 0.0) 4587888.0
4 1S1 2P1 (3)1( 1.0) 4588243.0
5 1S1 2P1 (3)1( 2.0) 4588974.0
6 1S1 2S1 (1)0( 0.0) 4594943.0
7 1S1 2P1 (1)1( 1.0) 4636124.0
8 1S1 3S1 (3)0( 1.0) 5343184.0
9 1S1 3P1 (3)1( 0.0) 5359516.0
10 1S1 3P1 (3)1( 1.0) 5359615.0
11 1S1 3P1 (3)1( 2.0) 5359816.0
12 1S1 3S1 (1)0( 0.0) 5360831.0
13 1S1 3D1 (3)2( 1.0) 5368693.0
14 1S1 3D1 (3)2( 2.0) 5368728.0
15 1S1 3D1 (3)2( 3.0) 5368792.0
16 1S1 3D1 (1)2( 2.0) 5369321.0
17 1S1 3P1 (1)1( 1.0) 5372722.0
-1
7.00 3 9.80+03 2.45+04 4.90+04 9.80+04 2.45+05 4.90+05 9.80+05 2.45+06 4.90+06 9.80+06 2.45+07 4.90+07 9.80+07
2 1 1.00-30 4.08-02 5.13-02 4.10-02 2.81-02 1.61-02 1.10-02 7.83-03 5.04-03 3.57-03 2.45-03 1.40-03 8.72-04 5.25-04 0.00+00
3 1 1.00-30 3.97-03 3.83-03 3.32-03 2.90-03 2.66-03 2.57-03 2.37-03 1.91-03 1.47-03 1.03-03 5.72-04 3.39-04 1.92-04 0.00+00
4 1 3.81+08 1.26-02 1.18-02 1.01-02 8.77-03 8.01-03 7.74-03 7.14-03 5.75-03 4.43-03 3.15-03 1.90-03 1.35-03 1.04-03-7.80-06
5 1 1.00-30 2.21-02 2.01-02 1.70-02 1.47-02 1.34-02 1.30-02 1.20-02 9.60-03 7.38-03 5.19-03 2.87-03 1.70-03 9.61-04 0.00+00
6 1 1.00-30 1.75-02 1.34-02 1.12-02 9.57-03 8.48-03 8.25-03 8.20-03 8.48-03 9.07-03 9.94-03 1.12-02 1.21-02 1.29-02 1.45-02
7 1 3.45+12 1.69-02 1.81-02 1.87-02 1.93-02 2.11-02 2.32-02 2.65-02 3.46-02 4.59-02 6.25-02 9.24-02 1.21-01 1.54-01-6.84-02
8 1 1.00-30 7.70-03 6.21-03 4.51-03 3.20-03 2.16-03 1.70-03 1.36-03 1.00-03 7.61-04 5.45-04 3.21-04 2.03-04 1.23-04 0.00+00
9 1 1.00-30 7.51-04 7.09-04 6.72-04 6.47-04 6.22-04 5.98-04 5.55-04 4.58-04 3.59-04 2.56-04 1.44-04 8.63-05 4.93-05 0.00+00
10 1 1.17+08 1.89-03 1.91-03 1.89-03 1.87-03 1.84-03 1.78-03 1.66-03 1.37-03 1.08-03 7.81-04 4.86-04 3.54-04 2.81-04-1.50-06
11 1 1.00-30 3.22-03 3.20-03 3.16-03 3.13-03 3.07-03 2.97-03 2.77-03 2.29-03 1.80-03 1.28-03 7.21-04 4.32-04 2.47-04 0.00+00
12 1 1.00-30 6.30-03 4.85-03 3.56-03 2.67-03 2.06-03 1.84-03 1.76-03 1.80-03 1.92-03 2.11-03 2.41-03 2.63-03 2.82-03 3.25-03
13 1 1.00-30 2.51-04 2.65-04 2.68-04 2.66-04 2.56-04 2.39-04 2.11-04 1.61-04 1.18-04 7.88-05 4.09-05 2.33-05 1.27-05 0.00+00
14 1 9.72+05 4.21-04 4.44-04 4.48-04 4.45-04 4.27-04 3.99-04 3.54-04 2.70-04 1.99-04 1.36-04 7.70-05 5.02-05 3.40-05 1.20-05
15 1 1.00-30 5.94-04 6.21-04 6.27-04 6.22-04 5.97-04 5.57-04 4.93-04 3.76-04 2.75-04 1.84-04 9.54-05 5.42-05 2.96-05 0.00+00
16 1 1.42+08 6.34-04 6.65-04 6.64-04 6.44-04 5.97-04 5.57-04 5.26-04 5.36-04 6.10-04 7.49-04 9.96-04 1.19-03 1.36-03 1.76-03
17 1 1.04+12 4.32-03 4.36-03 4.43-03 4.54-03 4.84-03 5.24-03 5.94-03 7.67-03 9.95-03 1.32-02 1.89-02 2.42-02 3.04-02-1.32-02
3 2 7.99+07 7.23-01 7.77-01 7.99-01 8.22-01 8.81-01 9.55-01 1.06+00 1.23+00 1.40+00 1.58+00 1.81+00 1.98+00 2.15+00-2.32-01
4 2 8.14+07 2.31+00 2.40+00 2.44+00 2.49+00 2.65+00 2.87+00 3.17+00 3.71+00 4.20+00 4.73+00 5.44+00 5.95+00 6.46+00-6.97-01
5 2 8.43+07 3.86+00 4.04+00 4.10+00 4.17+00 4.43+00 4.79+00 5.28+00 6.17+00 6.98+00 7.87+00 9.04+00 9.91+00 1.07+01-1.16+00
6 2 1.00-30 9.75-02 6.97-02 5.75-02 5.13-02 5.27-02 5.29-02 4.64-02 3.29-02 2.35-02 1.60-02 9.02-03 5.57-03 3.33-03 0.00+00
7 2 5.26+04 6.92-02 7.32-02 7.41-02 8.11-02 1.05-01 1.11-01 9.51-02 6.03-02 3.80-02 2.25-02 1.08-02 6.43-03 4.12-03-7.98-05
8 2 1.00-30 4.87-01 4.07-01 3.20-01 2.58-01 2.17-01 2.06-01 2.05-01 2.14-01 2.23-01 2.31-01 2.39-01 2.44-01 2.46-01 2.50-01
9 2 4.97+10 3.35-02 2.93-02 2.57-02 2.35-02 2.30-02 2.47-02 2.91-02 4.13-02 5.67-02 7.77-02 1.13-01 1.45-01 1.79-01-5.66-02
```

Excitation generation : ICFT script

This is a **perl** script, that runs the R-matrix suite of codes from the atomic structure through to a Maxwellian averaged collision strengths (adf04) file without further user input.

(Dr Whiteford, Dr Witthoeft, Dr Loch and myself)

It does allow for various optimisations both in terms of the atomic structure and the collisional calculation, but minimally **only requires the user to provide a list of configurations.**

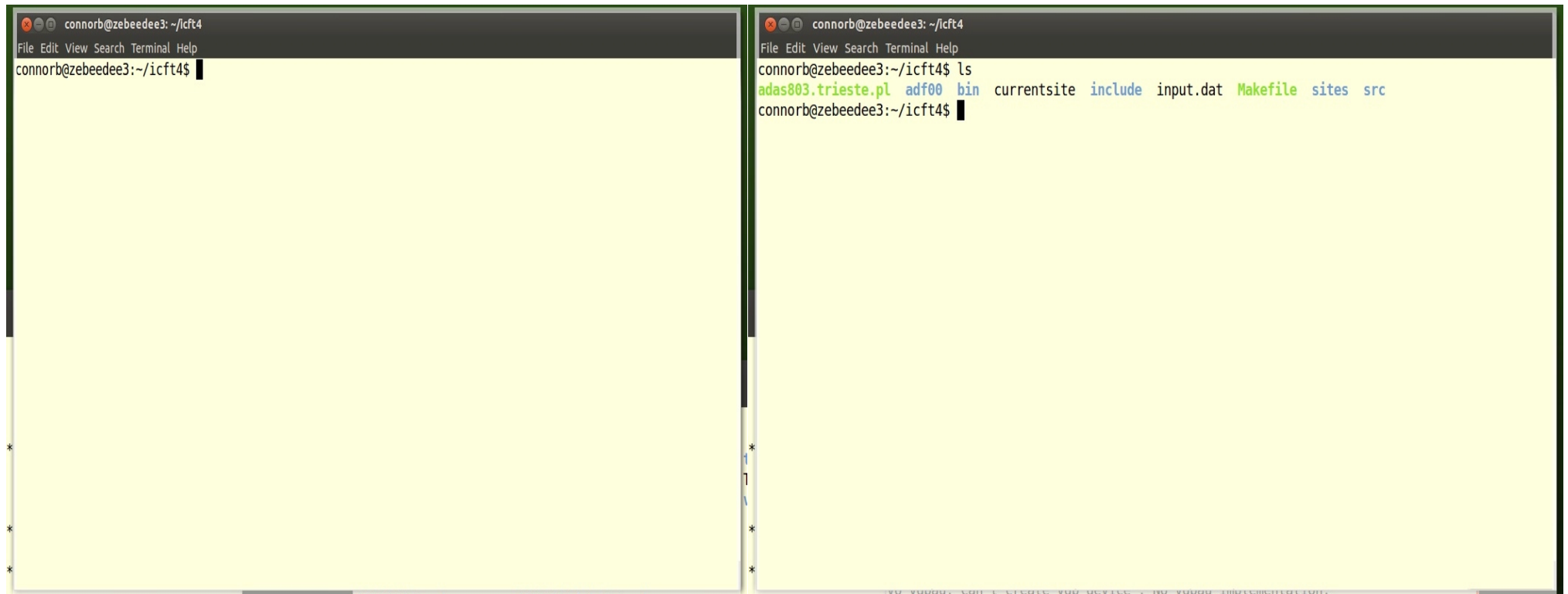
This allows for the efficient calculation along iso-electronic sequences, and been carried out for FI-like, Neon-like , B-like sequences by Dr Liang and others.

The script is also the foundation of our Monte Carlo error sensitivity, which I will discuss later.

ICFT script: Acquisition and installation

Acquire

Install



The image displays two terminal windows side-by-side, illustrating the steps to acquire and install the ICFT script. Both windows are titled 'connorb@zebeedee3: ~/icft4' and have a menu bar with 'File Edit View Search Terminal Help'.

The left terminal window shows the acquisition step, with the prompt 'connorb@zebeedee3:~/icft4\$' and a cursor waiting for input.

The right terminal window shows the installation step. It displays the command 'ls' followed by the output of the directory listing:

```
connorb@zebeedee3:~/icft4$ ls
adas803.trieste.pl  adf00  bin  currentsite  include  input.dat  Makefile  sites  src
connorb@zebeedee3:~/icft4$
```

ICFT script: Use (example)

```
connorb@zebeedee3: ~/icft4
File Edit View Search Terminal Help
maxc = 35
mesh_fine = 0.000325
mesh_coarse = 0.01
maxe/ionpot = 3
rdamp = 0
adamp = 0
accel = 0

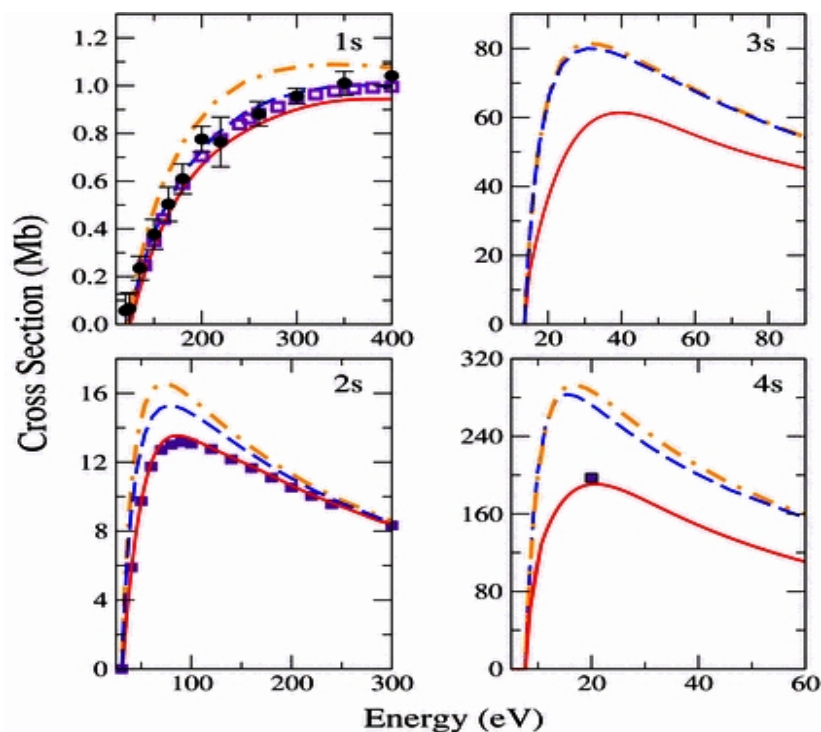
CONFIGURATION LIST
ls2
ls1 2s1
ls1 2p1
ls1 3s1
ls1 3p1
ls1 3d1
ls1 4s1
ls1 4p1
ls1 4d1
ls1 4f1
*
SCALING PARAMETERS
ls = 1.0
connorb@zebeedee3:~/icft4$ vi input.dat
*
connorb@zebeedee3:~/icft4$ ls
adas803.trieste.pl  adf00  bin  currentsite  include  input.dat  Makefile  sites  src
*
connorb@zebeedee3:~/icft4$
```

R-matrix/RMPS : ionisation

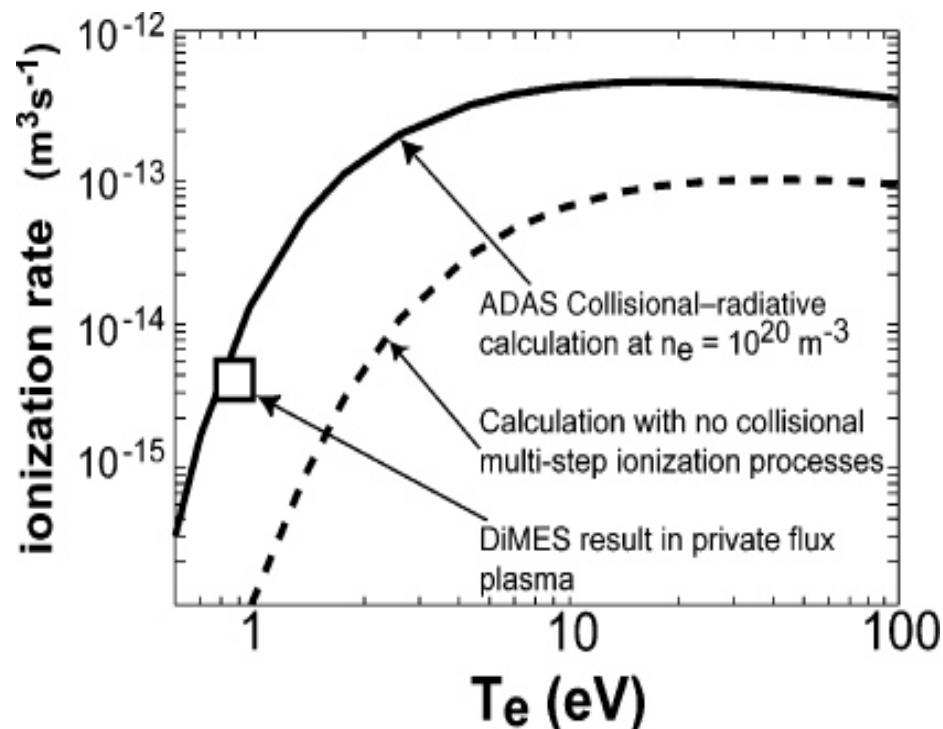
We have the capability to calculate electron-impact ionisation (ground & metastable) for light to mid-Z elements. With the availability of Prof Badnell's DRMPS (Dirac R-matrix with Pseudo-States) code, the heavier elements are now feasible.

It is the accuracy of the excited states that can prove problematic

Neutral Hydrogen



Neutral Lithium Effective Ionisation



Ultimately, the electron-impact excitation and ionisation are **both** required if we to produce Generalised Collisional Radiative (GCR) coefficients that are both temperature and density dependent.

Generalized collisional-radiative (GCR) coefficients

- Effective ionization rates

$$S_{CD,\sigma \rightarrow v} = \mathcal{I}_{v\sigma} - \sum_{j=1}^O \mathcal{I}_{vj} \sum_{i=1}^O \mathcal{C}_{ji}^{-1} \mathcal{C}_{i\sigma}$$

Ionization rates

CR matrix elements

- Effective recombination rates

$$R_{CD,v \rightarrow \sigma} = \mathcal{R}_{\sigma v} + \sum_{j=1}^O \mathcal{C}_{\sigma j} \sum_{i=1}^O \mathcal{C}_{ji}^{-1} \mathcal{R}_{iv}$$

- Total Line Power Loss

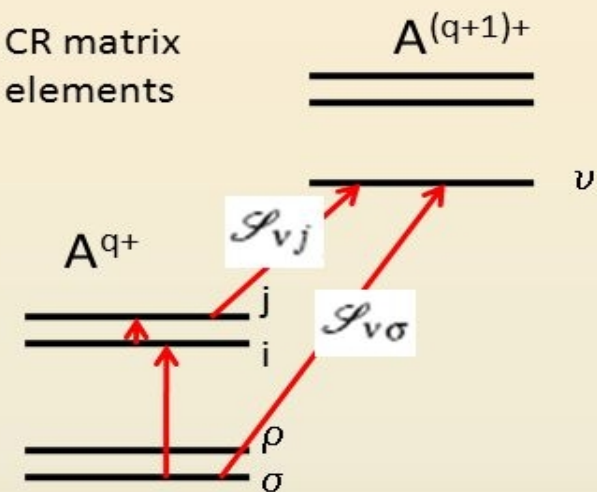
$$P_{LT,\sigma} = \sum_{k,j} \Delta E_{kj} A_{j \rightarrow k} F_{j\sigma}^{exc}$$

RR and DR rates

excitation rates

j->k transition energy

spontaneous emission rates



Effective ionization rate coefficient vs density and electron temperature

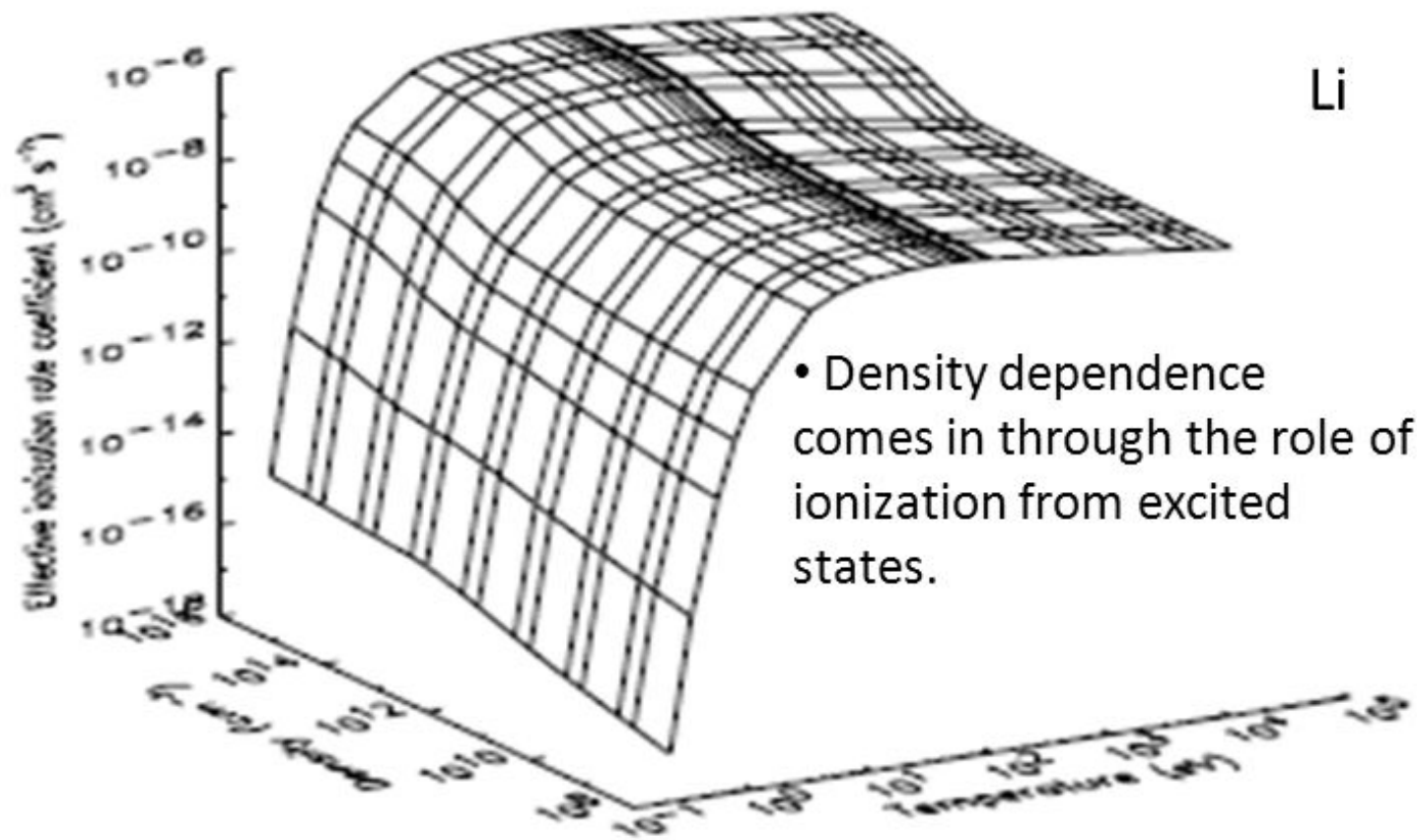


Fig. 8. Effective ionization rate coefficient for the ionization process $e + \text{Li}(1s^2 2s^2 S) \rightarrow \text{Li}^+(1s^2 S) + 2e$ as a function of electron temperature and density. Note that the density dependence comes in through the role of ionization from excited states.

Loch et al., ADNDT, 92 813 (2006)

Uncertainty in Theoretical Calculations

ICFT script

Baseline Studies

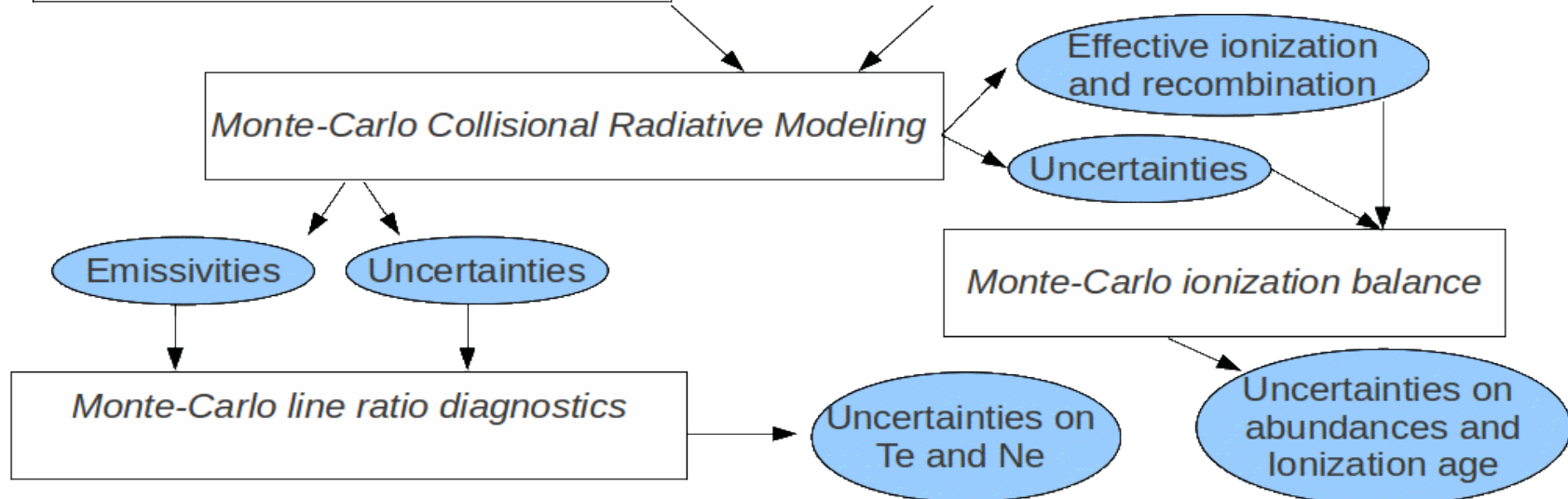
- Uncertainty is quantified as the difference between different theoretical approaches
- Representative of differences in the literature
- Quickly provides a generous uncertainty on an atomic dataset, while providing the correct temperature and density trends of more elaborate calculations.
- May not reflect the tighter constrained uncertainties derived from more elaborate calculations.
- Fundamental atomic structure and collisional rates remain uncorrelated.

Guides choices made in more elaborate models

Reassess the quality of the baseline rates and confirm baseline uncertainty range.

Sensitivity Studies

- Uncertainty is determined from the sensitivity of the calculation to key input parameters.
- Can produce fully correlated uncertainties.
- The objective choice of variation in the input parameters that reflects meaningful physical values remains difficult
- Does not determine the absolute uncertainty between methods.
- More time and resource intensive.



Current work for Molybdenum and Tungsten

Collaborators : Curtis Johnston, Stuart Loch, David Ennis
(Auburn)
: Steve Alan
(DIIID)

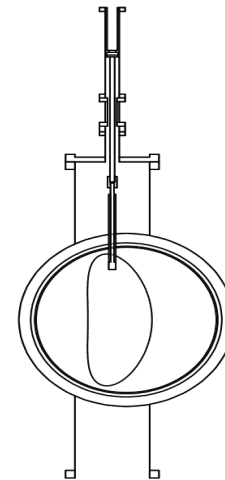
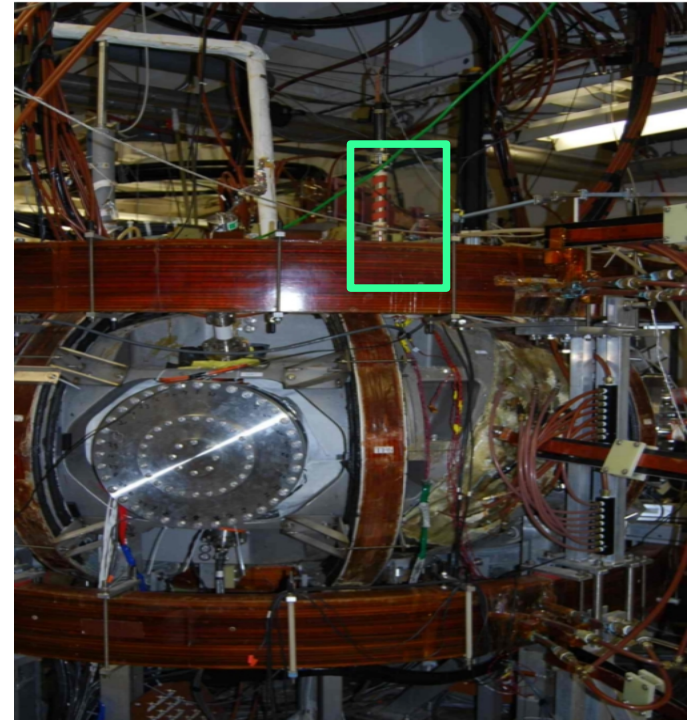
(i) Mo I/Mo II excitation and ionisation

(ii) W I excitation

Motivation

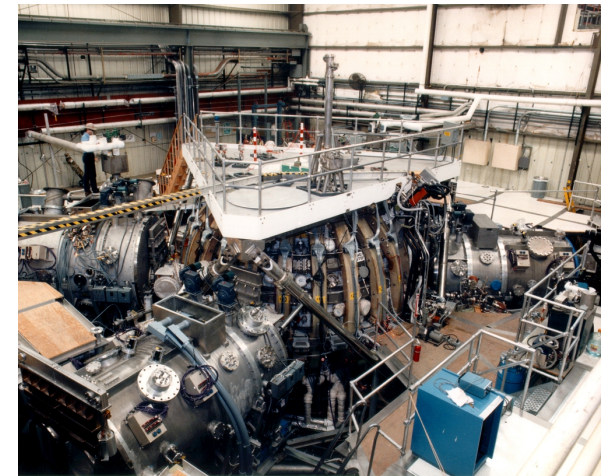
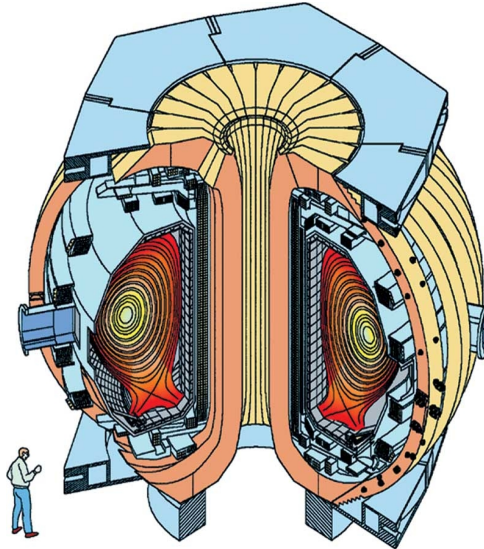
- Molybdenum/Tungsten employed in several fusion devices such as NSTX-U, DIII-D and EAST and CTH
- They have favourable physical properties such as high thermal conductivity

CTH (Auburn University)



Overview of DIII-D parameters

- Magnetic Field $B < 2.2$ T
- Major radius R 1.67 m
- Minor radius a 0.67 m
- Plasma Current < 3 MA
- Pulse duration < 7 s
- Majority ions Deuterium
- Temperatures and densities depend on chosen operating mode
- During metal tiles campaign
- Heating power < 26 MW for these experiments



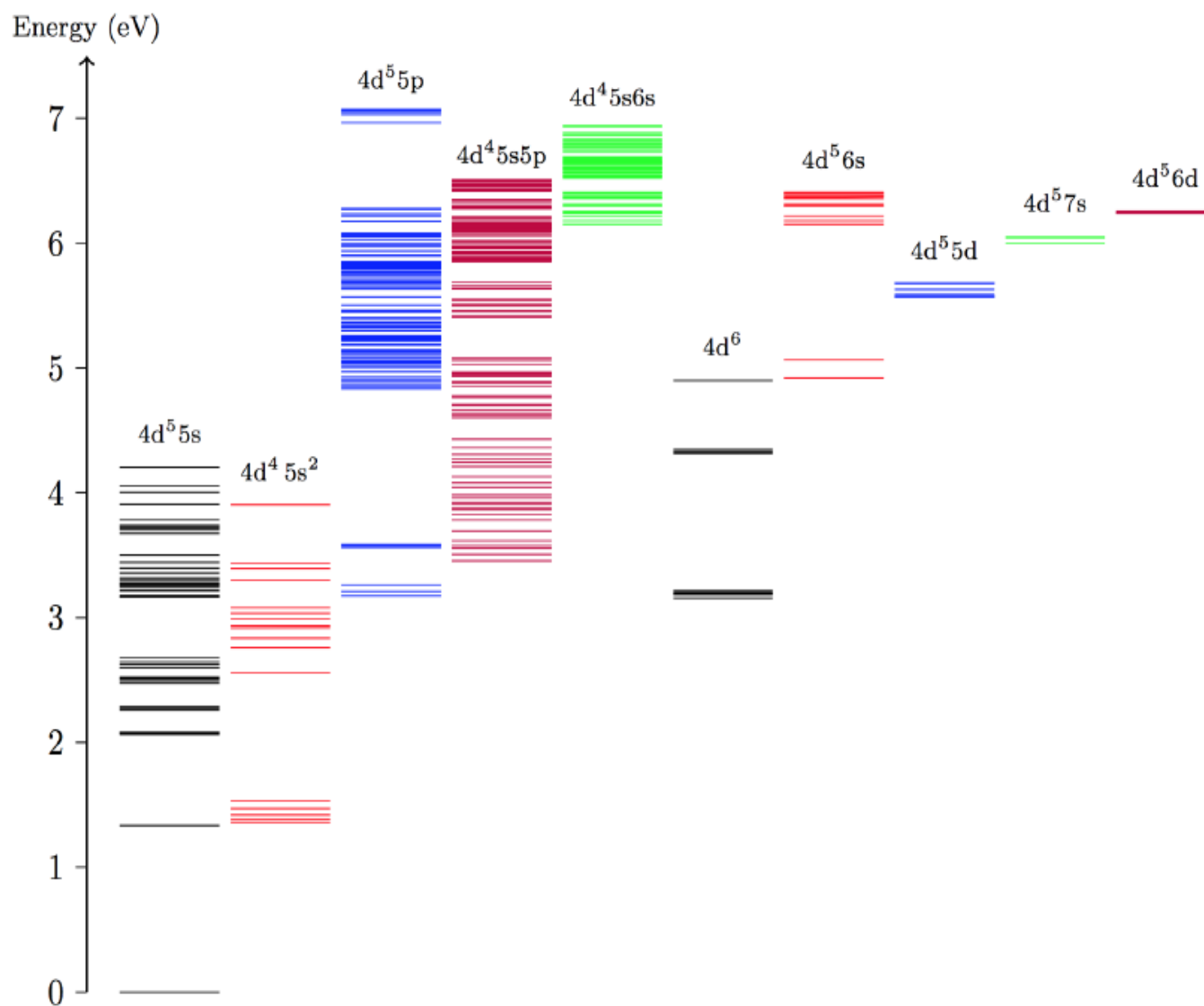


FIG. 1. Energy level spectrum of Mo I organised by electronic configuration. Each horizontal line designates a specific fine structure level listed in the NIST database.

λ (Å)	Transition $j - i$	A_{ji} (s^{-1})	
		Current	Whaling
3132.59	44 - 1	2.88×10^8	1.78×10^8
3170.34	42 - 1	2.76×10^8	1.36×10^8
3193.97	41 - 1	2.77×10^8	1.53×10^8
3456.39	35 - 1	4.93×10^6	4.20×10^6
3466.82	33 - 1	2.63×10^6	1.23×10^6
3798.26	28 - 1	7.56×10^7	6.90×10^7
3864.11	27 - 1	6.95×10^7	6.20×10^7
3902.96	26 - 1	6.55×10^7	6.17×10^7
4293.87	50 - 3	3.74×10^6	5.90×10^6
4326.74	49 - 4	3.19×10^6	4.50×10^6
4512.13	48 - 4	9.64×10^5	1.00×10^6
4524.33	49 - 6	2.42×10^6	1.76×10^6
4558.10	47 - 3	1.46×10^6	1.14×10^6
4576.49	48 - 5	3.10×10^6	2.14×10^6
4594.32	47 - 4	2.96×10^6	1.90×10^6
4626.45	49 - 7	6.62×10^6	4.00×10^6
4662.75	48 - 6	3.73×10^6	2.06×10^6
4979.12	39 - 2	1.38×10^6	2.30×10^6
5506.50	35 - 2	5.41×10^7	3.42×10^7
5533.03	33 - 2	5.47×10^7	3.59×10^7
5570.43	32 - 2	5.39×10^7	3.23×10^7
5632.46	32 - 3	3.18×10^6	7.16×10^6
5689.14	32 - 4	6.72×10^6	1.45×10^7
5650.14	33 - 4	1.41×10^6	1.58×10^6
5677.87	50 - 8	3.05×10^5	1.39×10^6
5689.14	32 - 4	6.72×10^6	1.45×10^7
5722.76	35 - 5	4.66×10^5	1.94×10^6
5751.42	33 - 5	4.76×10^6	4.30×10^6
5791.85	32 - 5	4.82×10^6	1.26×10^7
5858.28	35 - 6	2.57×10^6	5.93×10^6
5888.32	33 - 6	6.78×10^6	7.30×10^6

TABLE II. Table showing the radiative transition rates (in s^{-1}) obtained from the present model compared to experimental values given in [18]. The rates shown are obtained after shifting energies to experimental values.

We do have the experimental A-values From Whaling et al , and for such a complicated systems we have reasonable agreement between experiment and theory.

The lines below are categorized as strong diagnostic lines

- (i) $z^5P_{1,2,3}^o \rightarrow a^5S_2$ (557.0 nm, 553.3 nm, 550.6 nm)
- (ii) $z^7P_{2,3,4}^o \rightarrow a^7S_3$ (390.3 nm, 386.4 nm, 379.8 nm)
- (iii) $y^7P_{2,3,4}^o \rightarrow a^7S_3$ (319.4 nm, 317.0 nm, 313.3 nm)

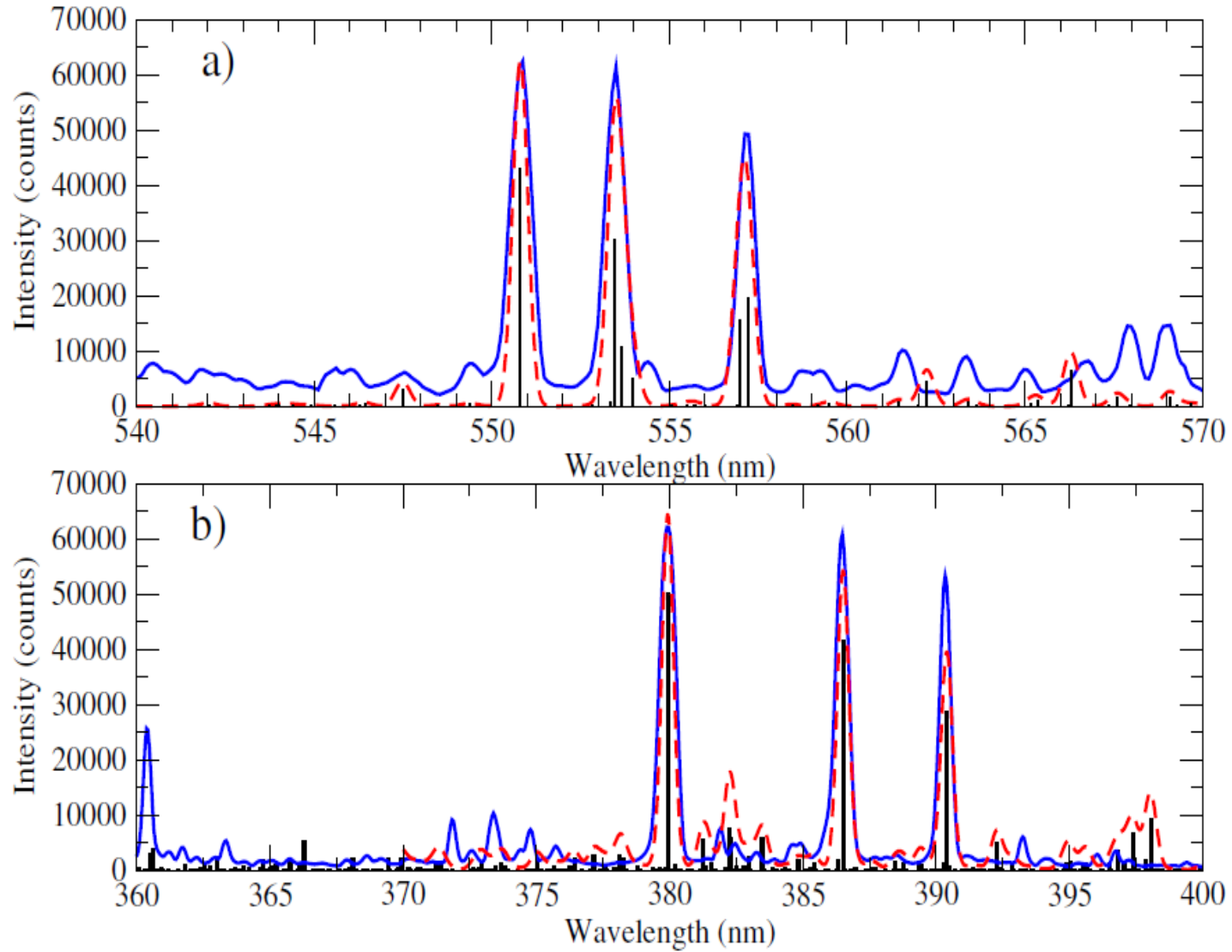
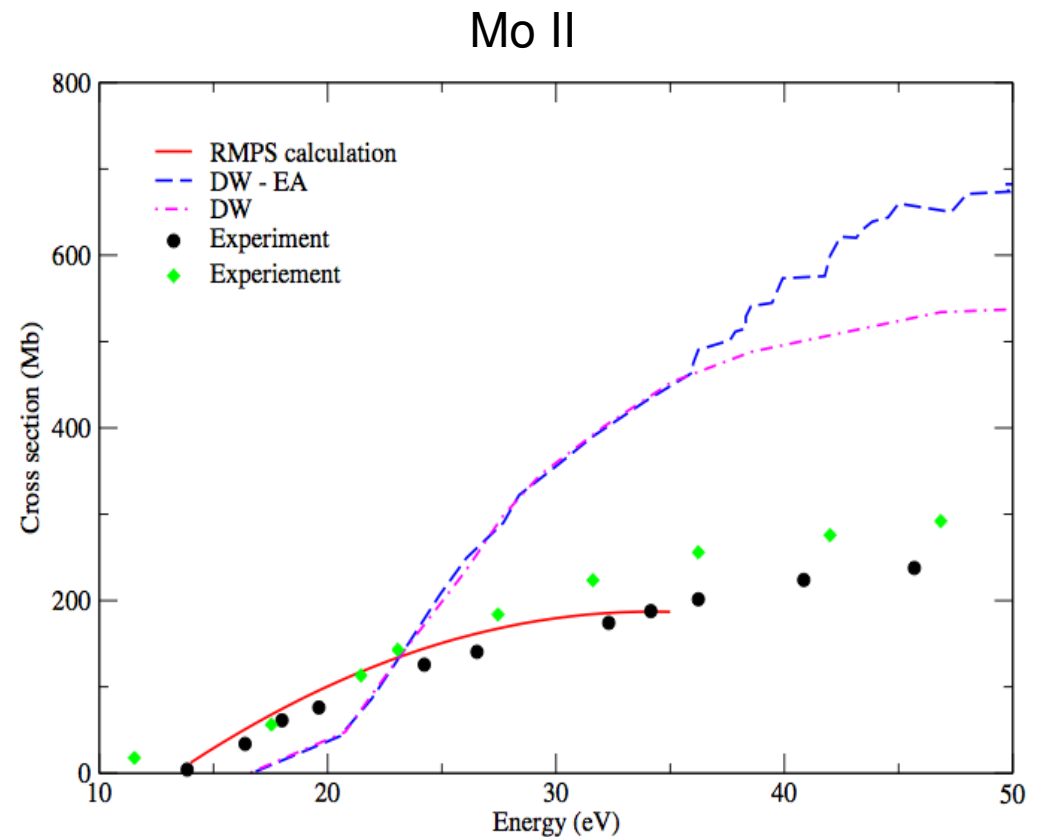
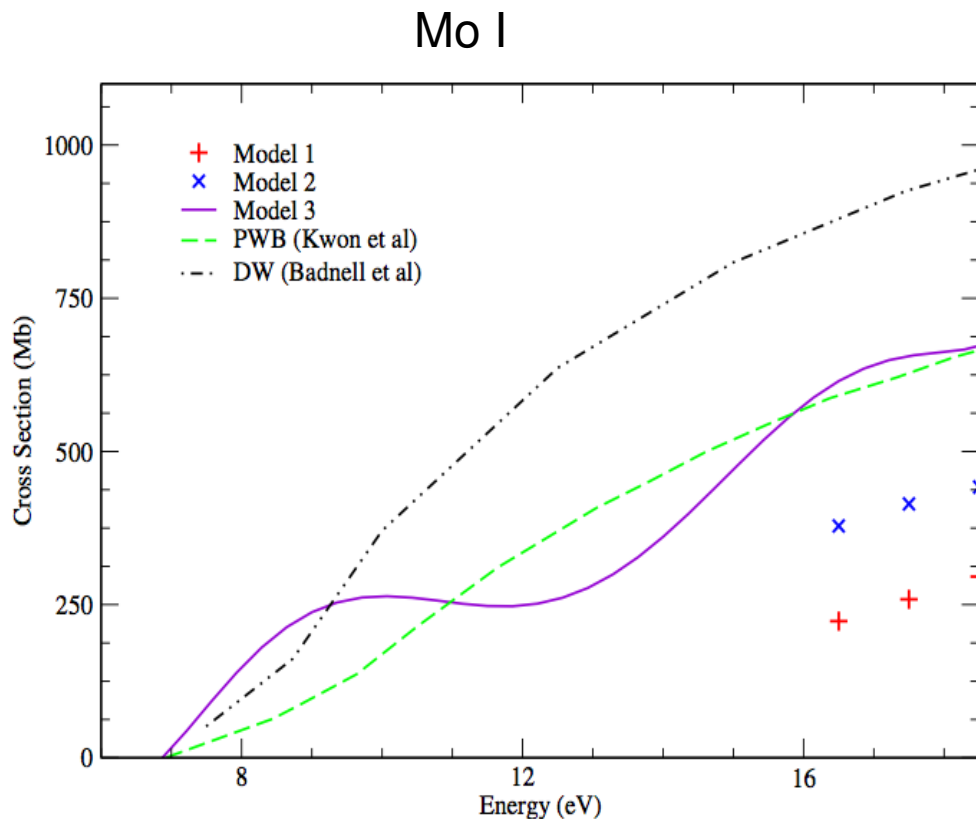


FIG. 6. Measured spectrum from the CTH plasma (solid blue line), compared with theoretical results. The solid black sticks show the PEC coefficients for the Mo I transitions, while the dashed red curve shows a theoretical spectrum based upon Gaussian convolved PEC data. A FWHM for the Gaussian convolution of 0.15 nm was used, based upon the instrument resolution, and the PECs are shown for an electron temperature of 6 eV and an electron density of $1 \times 10^{12} \text{ cm}^{-3}$.

RMPS : Mo I/Mo II ionization

- 1) Required multiple levels of parallelisation (by partial wave, also by Hamiltonian)
- 2) At 11,216 terms in the close-coupling expansion, probably the largest electron-impact carried out.

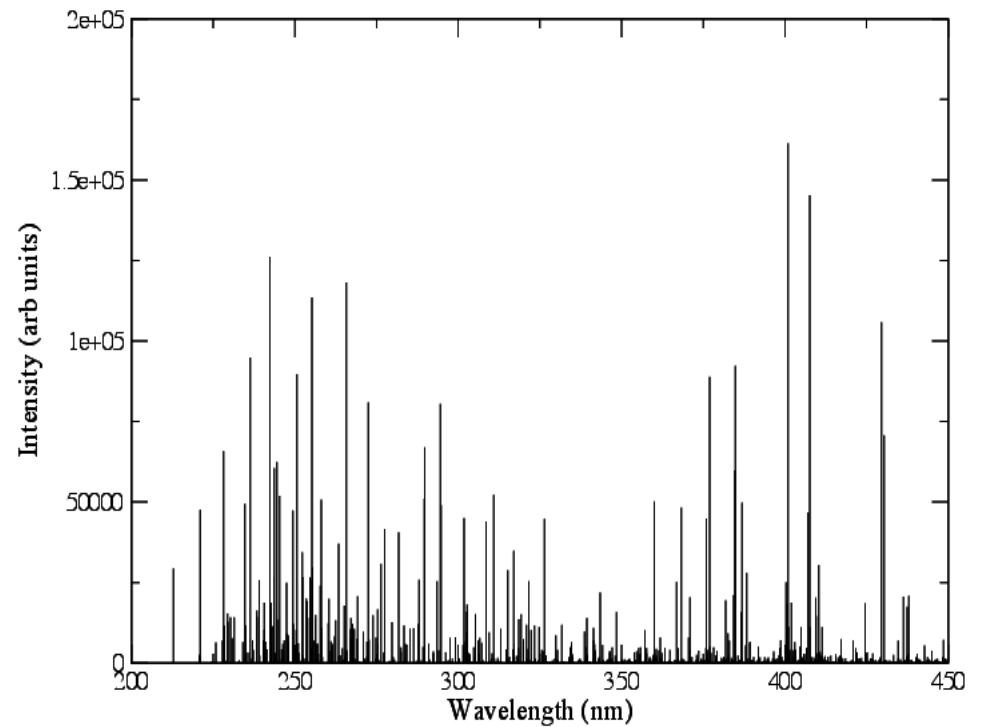
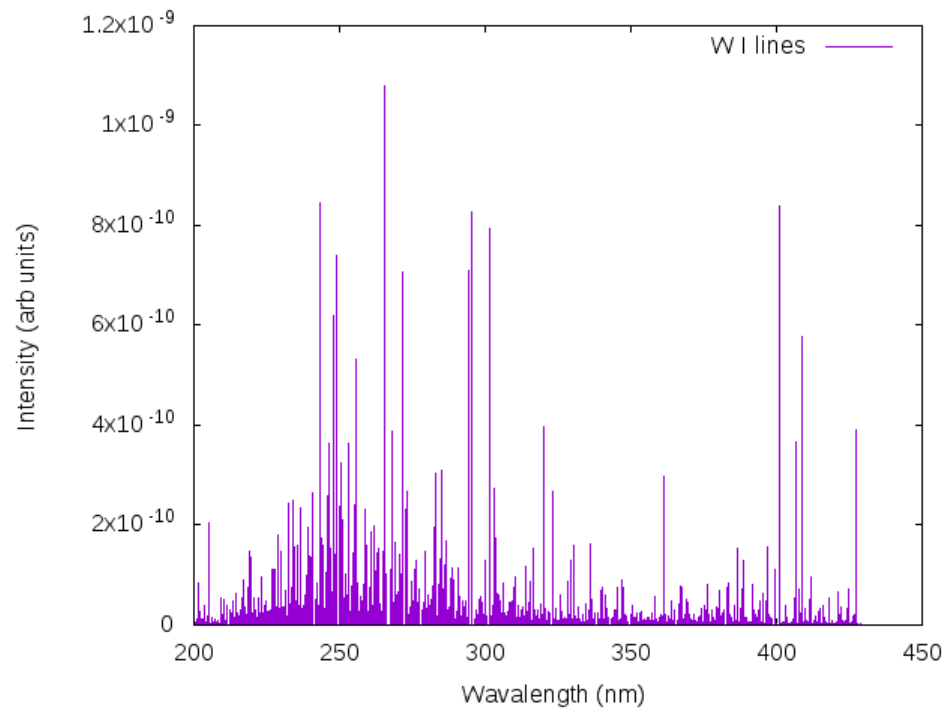


Tungsten

Currently, two WI adf04 files

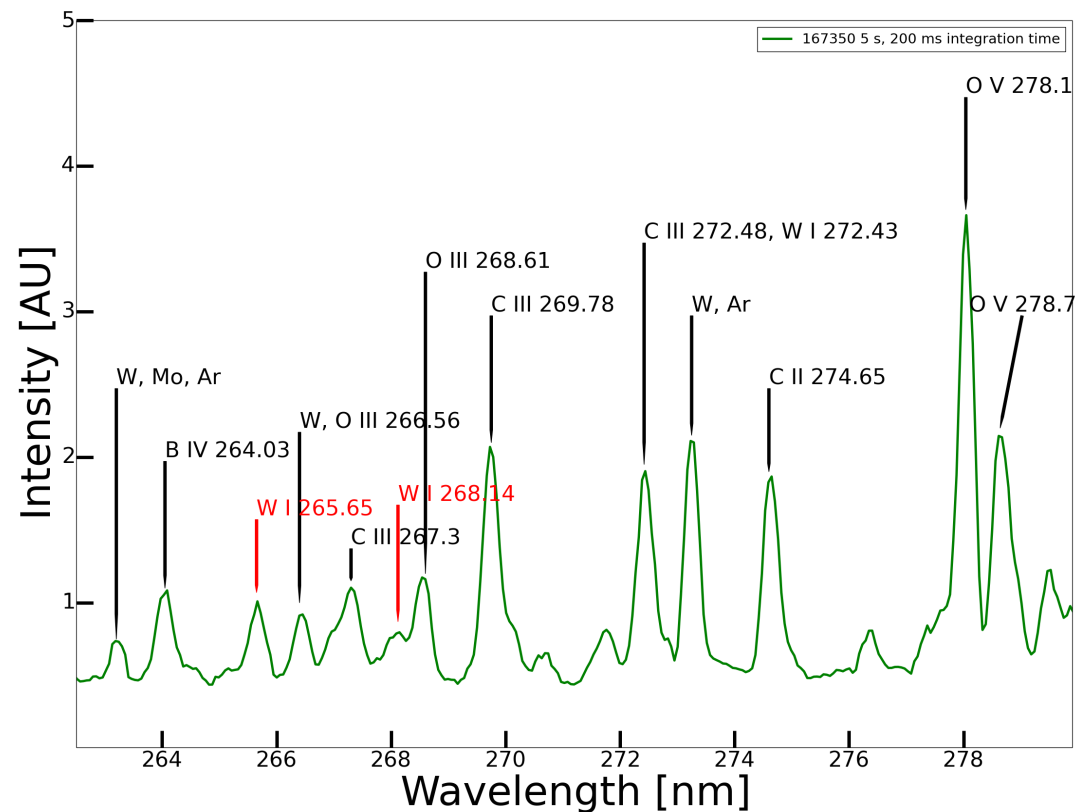
Cowan code, 3 configs in
the scattering plane-wave
Born calculation

GRASP + pDARC suite of R-matrix
Codes (24 configurations)



Overview of CTH measurements for Tungsten

- W I 265.65 nm observed to be on the order of the widely used 400.89 line:
 - Atomic calculations using ADAS confirm that W I 265.65 nm is strong for divertor temperatures and densities $\sim 10^{19} \text{ m}^{-3} \sim 10 \text{ eV}$
- Multiple W I lines in the region around 265.65 nm:
 - High density of lines in this region motivates higher resolution spectrometer/instrument



Ongoing and future Goals

- Development and use of R-matrix suite of codes for electron-impact excitation, ionisation and photoionisation.
- Focus on the near neutral systems but with the use of the ICFT script for comprehensive coverage
- Use of the Monte-Carlo perl script to provide and error file for each process
- Integration of data within magnetically-confined plasma databases such as ADAS, with conversion codes to facilitate integration into other formats.
- Integrate PhD (3) and post-doc(1) students into the group to continue the passing of knowledge.